Nano Research Energy

ISSN 2791-0091 (print); 2790-8119 (online)
https://doi.org/10.26599/NRE.2024.9120109

Research Article

Investigation into charge carrier dynamics in organic light-emitting diodes

Dong-Guang Zheng[1,§], Hyeon-Dong Lee[2,§], Gyeong Won Lee[3], Dong-Soo Shin[3], Jeongwon Kim[4], Jong-In Shim[3] (✉), Zhiqun Lin[5] (✉), Tae-Woo Lee[2,6] (✉), and Dong Ha Kim[4,7,8] (✉)

[1] *Information Engineering College, Hangzhou Dianzi University, Hangzhou 311305, China*
[2] *Department of Materials Science and Engineering, Seoul National University, 1 Gwanak-ro, Gwanak-gu, Seoul 08826, Republic of Korea*
[3] *Department of Photonics and Nanoelectronics, Hanyang University ERICA, 55 Hanyangdeahak-ro, Sangnok-gu, Ansan, Gyeonggi 15588, Republic of Korea*
[4] *Department of Chemistry and Nanoscience, Ewha Womans University, 52, Ewhayeodae-gil, Seodaemun-gu, Seoul 03760, Republic of Korea*
[5] *Department of Chemical and Biomolecular Engineering, National University of Singapore, 4 Engineering Drive 4, Singapore 117585, Singapore*
[6] *School of Chemical and Biological Engineering, Institute of Engineering Research, Research Institute of Advanced Materials, Soft Foundry, Seoul National University, 1 Gwanak-ro, Gwanak-gu, Seoul 08826, Republic of Korea*
[7] *Basic Sciences Research Institute (Priority Research Institute), Ewha Womans University, Seoul 03760, Republic of Korea*
[8] *Nanobio·Energy Materials Center (National Research Facilities and Equipment Center), Ewha Womans University, Seoul 03760, Republic of Korea*
[§] *Dong-Guang Zheng and Hyeon-Dong Lee contributed equally to this work.*

Received: 12 September 2023 / **Revised:** 13 November 2023 / **Accepted:** 22 November 2023

ABSTRACT

Organic light-emitting diodes (OLEDs) have demonstrated remarkable advancements in both device lifetime and luminous efficiency. However, insufficient operation lifetime due to device degradation remains a major hurdle, especially for brighter devices. Understanding the degradation mechanisms of OLEDs due to the degradation of functional materials and the formation of defects in device architectures continues to be a significant challenge. Herein, we evaluate the degradation characteristics by scrutinizing the electrical and optical properties, as well as analyzing the charge carrier dynamics in pristine and aged states of phosphorescent OLEDs (PhOLEDs). We show that degradation mechanisms in PhOLEDs can be elucidated in terms of the ideality factors of current and luminance in pristine and aged device states. The consistent shifts in distinct ideality factors across various states points out that the device degradation is attributed to the deterioration of the guest material, i.e. green-light-emitting phosphorescent material. Conversely, the incongruity in ideality factor changes between the two states indicates that the degradation results from the deterioration of non-light-emitting material. Subsequent characterization experiments provide further evidence that this degradation is primarily attributed to the deterioration of CBP-host material. The thorough understanding of degradation mechanisms established in this study can contribute to realing the highly reliable PhOLEDs with a long lifetime.

KEYWORDS

organic light-emitting diodes, ideality factor, carrier transport processes, degradation mechanism

1 Introduction

Organic light-emitting diodes (OLEDs) represent a class of popular lighting and display devices due to their ultra-thin structure, high efficiency, low power consumption, and flexible and bendable properties [1–6]. Based on those advantages, phosphorescent OLEDs (PhOLEDs) have been already commercialized as displays for TV and mobile. However, PhOLEDs with host-dopant systems still have lower stability compared to fluorescent OLEDs and require a complicated tandem structure improving device lifetime for commercialization, leading to high manufacturing costs. Therefore, it is still essential to deeply understand the underlying degradation mechanism in the host-dopant system to continuously improve the operation lifetime of OLED [7–10]. The intrinsic degradation of OLEDs is a highly complex phenomenon, as these devices typically consist of several functional layers, including the injection layer, transport layer, and emission layer. The inefficient charge carrier transport processes are induced by the degradation of functional materials and the formation of defects within the device layer under electrical stress [11–14]. Therefore, studying the physical processes

Address correspondence to Jong-In Shim, jishim@hanyang.ac.kr; Zhiqun Lin, z.lin@nus.edu.sg; Tae-Woo Lee, twlees@snu.ac.kr; Dong Ha Kim, dhkim@ewha.ac.kr

related to the charge carrier injection and transport plays a critical role in comprehending the degradation mechanisms of OLED devices [15–18].

In particular, host-guest system phosphorescent dye-doped OLEDs (PhOLEDs) have two distinct recombination and emission pathways in the emission layer (EML). One pathway involves exciton formation on the host material, followed by energy transfer to the guest material, known as Langevin recombination [19–22]. The other pathway is direct recombination on the guest material via charge carrier trapping, referred to as trap-assisted recombination [23–26]. These two mechanisms are mutually competitive in PhOLEDs and it is difficult to determine which mechanism is dominant. Identifying this mechanism may provide a crucial clue for achieving high-performance PhOLEDs. However, very little fundamental research has been conducted to address this issue.

Charge carrier dynamics in organic semiconductors have been widely investigated using electrical characterization techniques such as steady-state current density–voltage characteristics [27, 28], measurement in the time- or frequency-domain [29, 30], transient currents [31, 32], and impedance spectroscopy [33, 34]. Although these techniques effectively study the charge carrier dynamics, it is difficult to elucidate the degradation mechanisms related to exciton dynamics. Evaluation of the charge carrier distribution, including both transported and accumulated charges carriers, is therefore a crucial aspect in comprehending the correlations between charge carrier and exciton dynamics. In this context, we aim to link the luminance decay with its electrical characteristics via various characterization methods, establishing descriptive and easily understandable model for identifying, correlating, and quantifying the underlying degradation processes. Moreover, it investigates the impact of organic material degradation on charge carrier dynamics and exciton dynamics, ultimately influencing device performance and stability.

2 Experimental section/methods

2.1 Device fabrication

The constituent materials of the PhOLED devices are organized as follows. A 70 nm thick indium tin oxide (ITO) coated glass substrate is used as the anode. The polymeric gradient hole injection layers (GraHILs) consist of PEDOT:PSS (Poly(3,4-ethylenedioxythiophene)-poly (styrenesulfonate)) and PFI (Perfluoro-3, 6-dioxa-4-methyl-7-octene-1-sulfonic acid). For the hole transport layer (HTL), a 15 nm thick layer of TAPC (4,4'-cyclohexylidenebis [N, N-bis(4-methylphenyl) benzenamine]) is employed. As for the electron transport layer (ETL), a 55 nm thick layer of TPBi (2,2',2"-(1,3,5-Benzinetriyl)-tris(1-phenyl-1-H-benzimidazole)) is used. The double emission layers consist of TCTA and CBP, serving as the host materials for the emitting layers (each 5 nm). A green-light-emitting phosphorescent material, $Ir(ppy)_2(acac)$, is incorporated as the dopant material with a co-deposition of 3% with TCTA and 4% with CBP. These layers are sequentially deposited with appropriate thickness for the intended device structure by thermal evaporation. Lastly, lithium fluoride (1 nm) and aluminum (100 nm) layers are sequentially deposited on the ETL to form the cathode. The fabricated OLED devices are sealed by glass encapsulation by using a UV resin with a getter. The schematic of the fabricated OLED device is shown in Fig. 1(a), while Fig. 1(b) shows the EL process of multilayer PhOLED structure. As revealed by the ideality factor (see more details below), devices A and B with the same structure exhibit different optoelectronic characterization results, due to the degradation of guest and host materials, respectively. Holes and electrons are injected from the anode into the HTL and the cathode into the ETL, respectively. Subsequently undergoing charge carrier transport to the EML, recombining and forming excitons by the Coulomb force, resulting in light emission.

2.2 Device characterization

To comprehend the degradation mechanisms of PhOLED devices, we conducted optoelectronic measurements, i.e., the luminance-current density-voltage (*L–J–V*) characteristics and the EL spectra, using a source meter (Keithley 2602b) and a spectroradiometer (Minolta CS2000), respectively. The PhOLEDs were driven at a constant current density of 20 mA/cm^2 with monitored electrical and optical characteristics for device degradation study. Capacitance-voltage (*C–V*) characterizations were conducted by using an Agilent 4282A precision LCR meter with a frequency for the capacitance measurement of 1 kHz, with a modulating amplitude of 30 mV for observing the charge modulation. For electrical aging, the devices were driven with a constant current density (10 mA/cm^2) and characterized every 12 hours for all experiments described above. All experiments were carried out at room temperature. Interestingly, we discovered that while both devices A and B exhibited a similar degradation trend, they manifested distinct degradation mechanisms by analyzing ideality factors of current and luminance.

3 Results and discussion

3.1 *L–J–V* characteristics

The measurement of *L–J–V* and external quantum efficiency (EQE) characteristics under electrical stress for both devices are shown in Fig. 2 (Figs. S1–S3 in the Electronic Supplementary Material (ESM)). At the constant current density of 0.3 mA/cm^2, the operation voltage increases from 3.99 (0 h) to 6.56 V (72 h) (Fig. S1(a) in the ESM) and the luminance decreases from 345 (0 h) to 56 cd/cm^2 (72 h) (Fig. S2(a)) in device A; the operation voltage increases from 3.93 (0 h) to 5.36 V (72 h) (Fig. S1(b) in the ESM) and the luminance decreases from 356 to 154 cd/cm^2 (Fig. S2(b) in the ESM) in device B. The EQE changes between pristine and aged states for both devices are shown in Figs. 2(c) and 2(d), the values decrease from 27.1% and 27.5% to 18% and 21%, respectively. However, a simple analysis of electrical and optical characteristics is insufficient to provide a detailed degradation phenomenon.

To analyze in more depth, we study the carrier recombination mechanisms that impact the electrical and optical properties of PhOLED devices. In brief, the different mechanisms can be reflected in the *L–J–V* properties and the ideality factors characteristics of the devices, which can be described through the Shockley diode equation [35], given by

$$J = J_s[\exp(qV/\eta kT) - 1] \quad (1)$$

where q stands for the elementary charge, T is the absolute temperature, k is the Boltzmann constant, η is the ideality factor for the injection current, and J_s is the reverse saturation current density, J is the injection current density. The η value can be extracted from Eq. (1) as follows:

$$\eta = (q/kT)(\partial lnJ/\partial V)^{-1} \quad (2)$$

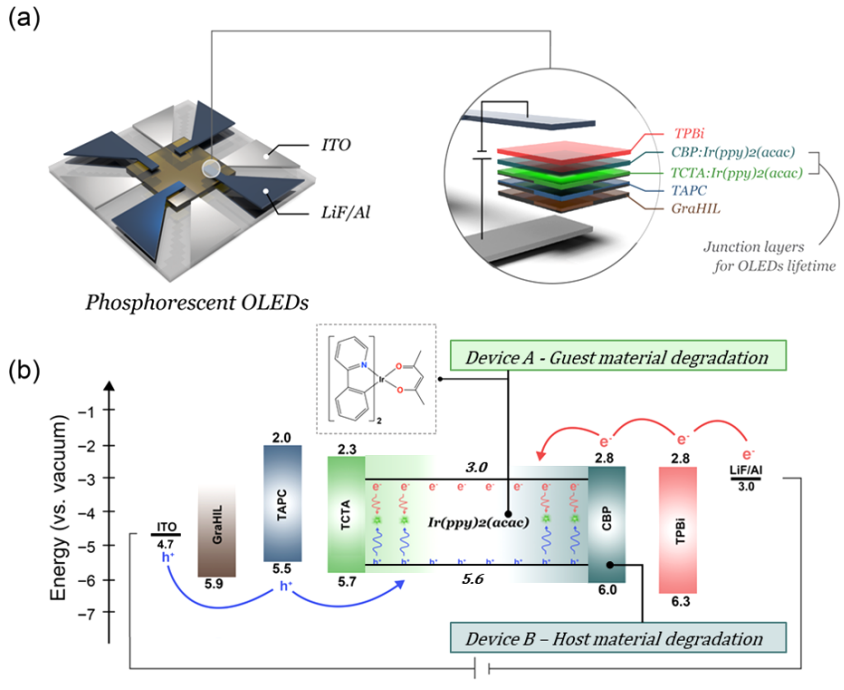

Figure 1 (a) Schematic of PhOLED material stack structure. (b) Energy level diagram of PhOLED.

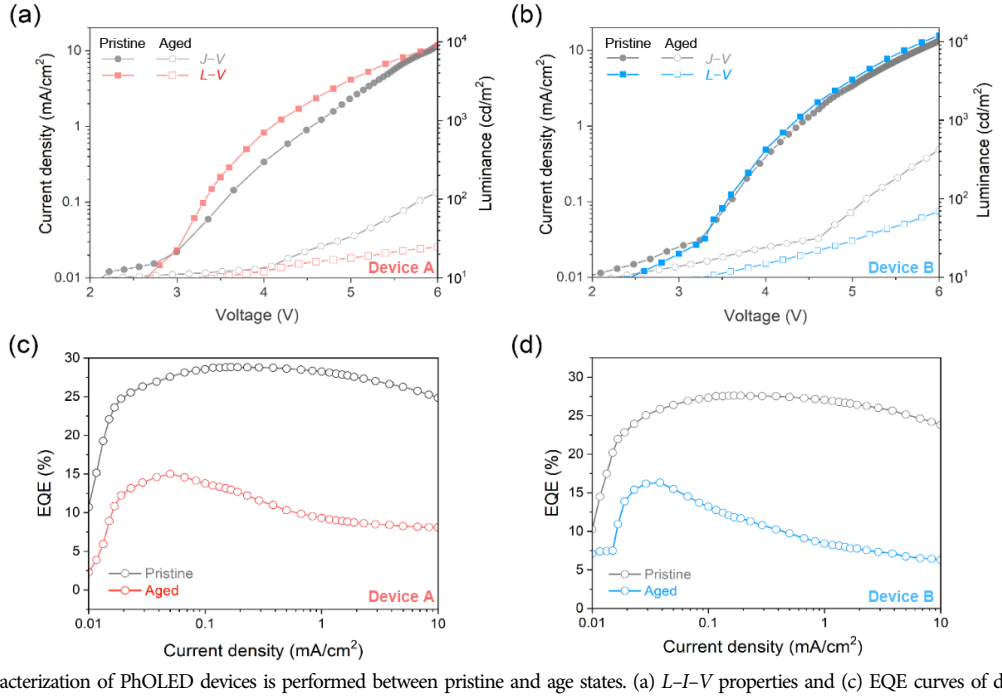

Figure 2 The characterization of PhOLED devices is performed between pristine and age states. (a) *L*–*I*–*V* properties and (c) EQE curves of device A. (b) *L*–*I*–*V* properties and (d) EQE curves of device B.

The η value in Eq. (2) can reflect the carrier transport and recombination in a device. The η value of 1 reveals bimolecular recombination (Langevin recombination) [22]. When the trap-assisted recombination competes with the bimolecular recombination, the η value typically falls within the range of 1 and 2 ($1 < \eta < 2$) [26]. If the trap-assisted recombination becomes dominant, the η value of 2 characterizes the Shockley-Read-Hall (SRH) recombination [22, 26, 36]. The existence of defects inside the PhOLED devices causes the ideality factor to significantly exceed 2, as reported in several articles [36, 37, 38].

The η curves in their pristine state for both devices are shown in Figs. 3(a) and 3(b) in the ESM. According to Table 1, the minimum η η_{iv} values are 2.66 and 3.15, respectively, which can be attributed to leakage current and/or trap-assisted recombination. However, in aged states, the determined η values increase significantly to 3.93 and 4.23, respectively, indicating the change in charge carrier transport and increase in defect density. Analysis of ideality factor η suggests an inefficient carrier injection and a severely deteriorated transport layer [26, 36, 37]. Electrically driven PhOLEDs convert electrical energy into light emission through charge carrier injection and radiative recombination. Thereby the recombination mechanisms can also be identified by the ideality factor from the luminance (η_{opt}) [26, 39–43]. In the EL characteristics, the luminance, L, presents an exponential dependence on voltage as follows:

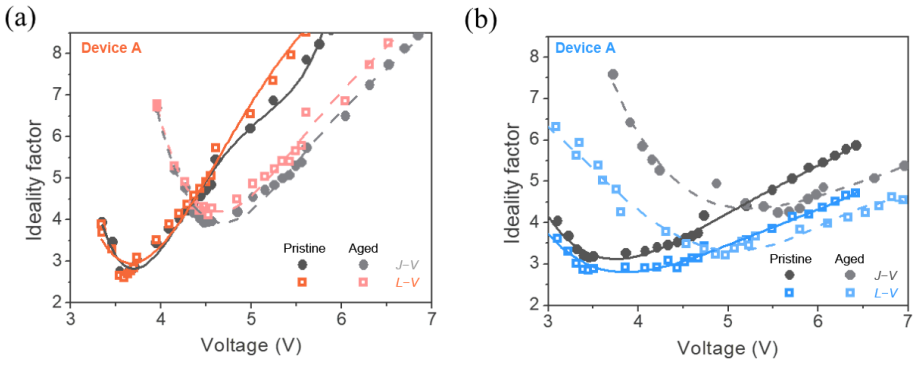

Figure 3 The ideality factors from the current density and luminance between pristine and aged states in (a) device A and (b) device B.

Table 1 Comparing ideality factor values from the current density and luminance between pristine and aged states

PhOLEDs	Minimum η value (V)		Minimum η_{opt} value (V)	
	Pristine	Aged	Pristine	Aged
Device A	2.66	3.93	2.59	4.11
Device B	3.15	4.23	2.84	3.20

$$L \propto \exp(qV/\eta_{opt}kT) \quad (3)$$

At low voltages, the ideality factor of luminance, η_{opt}, directly reflects the competition of various recombination processes, analogous to the case for the ideality factor of current. With the voltage increase, the light emission deviates from the exponential behavior, indicating that the injected current has reached the space-charge limit. The η_{opt} value determines the slope of the exponential luminance and can be directly obtained by numerical differentiation using the following equation:

$$\eta_{opt} = (q/kT)(\partial lnL/\partial V)^{-1} \quad (4)$$

The η_{opt} curves in their pristine state for both devices are also presented in Figs. 3(a) and 3(b) to allow for a comparison with the η curves. Referring to Table 1, the minimum η_{opt} values are 2.59 and 2.84, respectively, indicating that trap-assisted recombination is the dominant mechanism. Unlike the ideality factor of current, the significance of ideality factor of luminance lies in identifying radiative recombination processes. This suggests that the trap-assisted recombination, which occurs on the guest molecules, $Ir(ppy)_2(acac)$, acting as the trap-assisted recombination centers, is a radiative recombination process.

Following the electrical stress, the minimum η_{opt} value for device A rapidly increases to 4.11, implying that the increase in nonradiative recombination at the guest molecule sites due to the degradation of the guest molecules. In contrast, the minimum η_{opt} value increases to 3.20 for device B, which is much less than that of device A. Furthermore, the difference in the ideality factors of current and luminance for aged device B suggests that the degradation mechanism and position can be attributed to other organic materials. A thorough analysis of electrical and optical experiments will illuminate the degradation mechanism in device B.

3.2 Capacitance characteristics

The impedance characterizations (Figs. S4 and S5 in the ESM) of PhOLEDs provide detailed information on carrier injection, trap accumulation, and device degradation. The *C*–*V* characteristics of pristine and aged states for both devices are shown in Fig. 4. Qualitatively, both devices exhibit similar degradation tendencies, such as a decrease in peak capacitance (C_{peak}) and a shift of peak voltage (V_{peak}) towards a higher value.

The accumulation of space charges at the TCTA/TATC interface results in charged excitations, such as polarons or bipolarons, inducing dipole orientation and negative dipole moment formation. Holes can be easily injected into the EML through the GraHIL, even at 0 V or lower voltage [44–46]. TCTA and CBP act as host materials for the double-emitting layers. The deep highest occupied molecular orbital (HOMO) level (0.3 eV) and high lowest unoccupied molecular orbital (LUMO) level (0.5 eV) shown in Fig. 1(b) at the TCTA/CBP interface lead to charge carrier accumulation and hinder charge carrier movement. High hole mobility (3×10^{-4} $cm^2/(Vžs)$) and low electron mobility (10^{-8} $cm^2/(Vžs)$) of TCTA result in more holes moving and accumulating at the interface [47, 48]. Meanwhile, the higher energy barrier for electron injection and the perfect match of the LUMO energy level of TPBi and CBP facilitate electron injection into the CBP-host EML under higher voltage bias, which combines with accumulated holes on the light emitter band-energy level. The capacitance change depends on the relative rates of electron injection and consumption. If the electron injection rate is slower than the consumption rate, the capacitance increases; otherwise, it decreases [30, 33, 45].

Both aged devices demonstrate V_{peak} shift towards a higher value, indicating decline in carrier injection and/or transport ability due to device degradation. The degradation products of the TCTA host material are the primary contributors to the formation of hole traps and exciton loss [49–51]. However, the determination of V_{dh} shift is carried out by evaluating the fitting CV curves within the hole injection region. In device A, the V_{dh} values between the pristine and aged states appeared at –0.8 V, and the capacitance increment caused by hole injection is lower than that of the pristine device, even at a higher voltage in Fig. 4(a). This discrepancy is not consistent with the anticipated degradation of TCTA host material. It suggests that the degradation occurs on the guest molecules. The degraded guest molecules no longer contribute to light emission and act instead as charge-trapping sites and nonradiative recombination centers, which affect charge carrier mobility and transport properties, resulting in reduction of capacitance increment.

In the device B, it is notable that the V_{dh} values exhibit shift

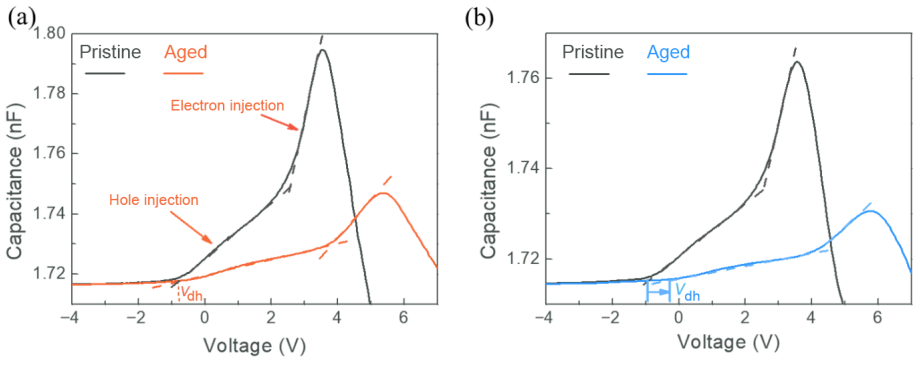

Figure 4 The capacitance-voltage characteristics between pristine and aged states in (a) device A and (b) device B.

trend from –0.9 V of pristine state to –0.2 V of aged state. Moreover, we also conducted fittings for the CV curves of electron injection regions in both devices. After comparison, the value of the relative change in the slope between pristine and aged states, 0.0057 of device A is nearly equivalent to 0.0054 of device B in the hole injection region. Nevertheless, when considering the value of the relative change in the slope in the electron injection region, the value of device B (0.041) is greater than that of device A (0.025). This observation suggests that the decline of hole injection ability is influenced by decomposition of GraHILs [48], while the deterioration of electron injection is attributed to the formation of charge carrier traps at the CBP host EML and/or CBP host EML/ETL interface, which simultaneously suppress electron injection. The degradation products of CBP host molecules not only act as trap sites where electrons or holes can reside but also provide nonradiative recombination centers as well as exciton-polaron quenching sites. Compared to device A, degraded device B experiences a more significant impact on carrier injection and transport properties due to the formation of traps.

3.3 EL characteristics

We compare the normalized EL spectra of pristine and aged states for both devices in Fig. 5 (Fig. S6 in the ESM). While device A exhibits little change in EL spectra (Fig. 5(a)), the EL spectra from device B undergo a red-shift and broadening due to the strengthening of a shoulder peak (Fig. 5(b)). This change in the EL spectra is generally attributed to a shift in the recombination zone within the EML. In pristine devices, the recombination zone is confined at the TCTA/CBP interface due to the deep HOMO level and high LUMO level at the interface. The consistency of the EL spectra in device A indicates that the degradation of the guest molecules does not lead to a shift in the recombination zone. In the aged device B, the change in steepness of the capacitance curve (Fig. 4(b)) induced by electron injection is greater than that in device A, implying that the accumulation of free electron density in the CBP host-EML becomes less. In general, free radical species—degradation products, which serve as intermediates in the proposed degradation mechanism, possess a singly occupied molecular orbital (SOMO) level within the CBP HOMO-LUMO gap. Consequently, they are anticipated to undergo facile oxidation or reduction by charge carriers. These radicals may function as deep charge traps, leading to the manifestation of internal fixed charge when filled and thus leads to a rise of operating voltage. [52–54]. Furthermore, the degradation products derived from the CBP host material also function as nonradiative recombination centers and exciton quenchers, leading to a luminance loss. It is important to highlight that the single degradation product originating from the CBP host material may simultaneously serve as a carrier trap as well as a quenching site. Thus, the degradation products act as charge traps, exciton quenchers, and nonradiative recombination centers, causing the imbalance of charge carriers in EML, which results in shift in the recombination zone [48, 55, 56].

4 Conclusions

In this study, we have established a protocol to identify the underlying degradation mechanism that occurs under electrical stress via analysis of the electrical and optical characteristics of PhOLEDs. The distinct impacts of the degradation of different organic materials on charge carrier and exciton dynamics have been demonstrated. Analysis of the quantitative factors, such as the ideality factors obtained from the *L*–*I*–*V* characteristics, has indicated that the change in charge carrier transport and accumulation properties within the EML may be responsible for device degradation. It is conjectured that, after electrical stress, the degradation of PhOLEDs with an identical architecture can be caused by diverse degradation mechanisms. This variation may be attributed to the formation of distinct degradation products through electrochemical reactions involving various organic

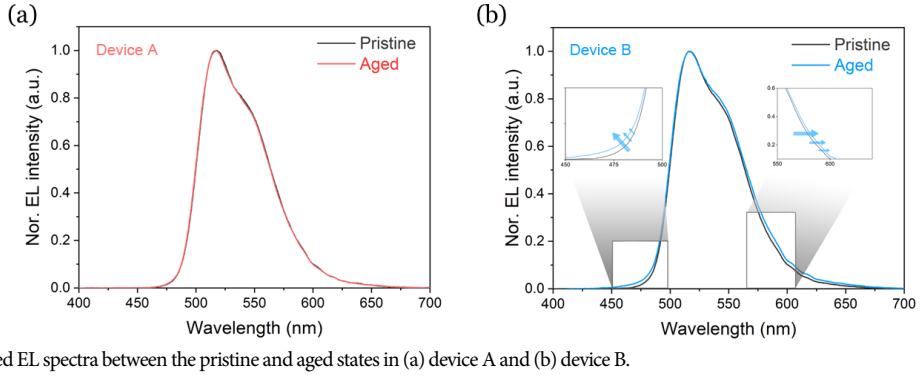

Figure 5 The normalized EL spectra between the pristine and aged states in (a) device A and (b) device B.

functional materials, consequently influencing the charge carrier distribution in the EML. Furthermore, all the resulting byproducts directly or indirectly contribute to the degradation of the electrical and optical performance of PhOLEDs. The comparison between ideality factors of current and luminance provides a straightforward and powerful means of comprehending the charge carrier and exciton dynamics for deducing the physical model that underpins the degradation phenomenon. This thorough understanding of degradation mechanisms may be beneficial for enabling highly reliable PhOLEDs with a long lifetime.

Acknowledgements

This work was supported by the National Research Foundation of Korea (NRF) grant funded by the Korean Government (2020R1A2C3003958), the Basic Science Research Program (Priority Research Institute) through the NRF grant funded by the Ministry of Education (2021R1A6A1A10039823), and the Korea Basic Science Institute (National Research Facilities and Equipment Center) grant funded by the Ministry of Education (2020R1A6C101B194).

Electronic Supplementary Material: Supplementary material (please send us a short summary regarding the Supporting info, thanks) is available in the online version of this article at https://doi.org/10.26599/NRE.2024.9120109.

Declaration of conflicting interests

The authors declare no conflicting interests regarding the content of this article.

Data availability

All data needed to support the conclusions in the paper are presented in the manuscript and/or the Supplementary Materials. Additional data related to this paper may be requested from the corresponding author upon request.

References

[1] Meerheim, R.; Walzer, K.; Pfeiffer, M.; Leo, K. Ultrastable and efficient red organic light emitting diodes with doped transport layers. *Appl. Phys. Lett.* **2006**, *89*, 061111.

[2] Gustafsson, G.; Cao, Y.; Treacy, G. M.; Klavetter, F.; Colaneri, N.; Heeger, A. J. Flexible light-emitting diodes made from soluble conducting polymers. *Nature* **1992**, *357*, 477–479.

[3] Kwon, O. E.; Shin, J. W.; Oh, H.; Kang, C. M.; Cho, H.; Kwon, B. H.; Byun, C. W.; Yang, J. H.; Lee, K. M.; Han, J. H. et al. A prototype active-matrix OLED using graphene anode for flexible display application. *J. Inf. Disp.* **2020**, *21*, 49–56.

[4] Tessler, N.; Harrison, N. T.; Friend, R. H. High peak brightness polymer light-emitting diodes. *Adv. Mater.* **1998**, *10*, 64–68.

[5] Li, W.; Li, Y. Q.; Shen, Y.; Zhang, Y. X.; Jin, T. Y.; Chen, J. D.; Zhang, X. H.; Tang, J. X. Releasing the trapped light for efficient silver nanowires-based white flexible organic light-emitting diodes. *Adv. Opt. Mater.* **2019**, *7*, 1900985.

[6] Laäaäperi, A.; Hyytiäinen, I.; Mustonen, T.; Kallio, S. 30.1: *Invited Paper*: OLED lifetime issues in mobile phone industry. *SID Symp. Dig. Tech.* **2007**, *38*, 1183–1187.

[7] Seo, Y.; Na, I.; Kim, Y.; Chae, H.; Oh, K.; Yang, J.; Yoon, S.; Joo, M. K. Degradation pattern of contact resistance and characteristic trap energy in blue organic light-emitting diodes. *Org. Electron.* **2021**, *91*, 106067.

[8] Hauenstein, C.; Gottardi, S.; Torun, E.; Coehoorn, R. ; van Eersel, H. Identification of OLED degradation scenarios by kinetic Monte Carlo simulations of lifetime experiments. *Front. Chem.* **2022**, *9*, 823210.

[9] Salameh, F.; Al Haddad, A.; Picot, A.; Canale, L.; Zissis, G.; Chabert, M.; Maussion, P. Modeling the luminance degradation of OLEDs using design of experiments. *IEEE Trans. Ind. Appl.* **2019**, *55*, 6548–6558.

[10] Tyagi, P.; Srivastava, R.; Giri, L. I.; Tuli, S.; Lee, C. Degradation of organic light emitting diode: Heat related issues and solutions. *Synth. Met.* **2016**, *216*, 40–50.

[11] Bangsund, J. S.; Hershey, K. W.; Holmes, R. J. Isolating degradation mechanisms in mixed emissive layer organic light-emitting devices. *ACS Appl. Mater. Interfaces* **2018**, *10*, 5693–5699.

[12] Ha, D. G.; Tiepelt, J.; Fusella, M. A.; Weaver, M. S.; Brown, J. J.; Einzinger, M.; Sherrott, M. C.; Van Voorhis, T.; Thompson, N. J.; Baldo, M. A. Dominance of exciton lifetime in the stability of phosphorescent dyes. *Adv. Opt. Mater.* **2019**, *7*, 1901048.

[13] Yang, R. Y.; Li, X. M.; Cao, X. A. Role of wide bandgap host in the degradation of blue phosphorescent organic light-emitting diodes. *J. Appl. Phys.* **2017**, *122*, 075501.

[14] Yang, K.; Nam, S.; Kim, J.; Kwon, E. S.; Jung, Y.; Choi, H.; Kim, J. W.; Lee, J. Effects of charge dynamics in the emission layer on the operational lifetimes of blue phosphorescent organic light-emitting diodes. *Adv. Funct. Mater.* **2022**, *32*, 2108595.

[15] Negi, S.; Mittal, P.; Kumar, B. Impact of different layers on performance of OLED. *Microsyst. Technol.* **2018**, *24*, 4981–4989.

[16] Chulkin, P.; Vybornyi, O.; Lapkowski, M.; Skabara, P. J.; Data, P. Impedance spectroscopy of OLEDs as a tool for estimating mobility and the concentration of charge carriers in transport layers. *J. Mater. Chem. C* **2018**, *6*, 1008–1014.

[17] Negi, S.; Mittal, P.; Kumar, B. Analytical modelling and parameters extraction of multilayered OLED. *IET Circuits, Devices Syst.* **2019**, *13*, 1255–1261.

[18] Schober, M.; Anderson, M.; Thomschke, M.; Widmer, J.; Furno, M.; Scholz, R.; Lüssem, B.; Leo, K. Quantitative description of charge-carrier transport in a white organic light-emitting diode. *Phys. Rev. B* **2011**, *84*, 165326.

[19] Grüne, J.; Bunzmann, N.; Meinecke, M.; Dyakonov, V.; Sperlich, A. Kinetic modeling of transient electroluminescence reveals TTA as an efficiency-limiting process in exciplex-based TADF OLEDs. *J. Phys. Chem. C* **2020**, *124*, 25667–25674.

[20] Peng, X. M.; Qiu, W. D.; Li, W. Q.; Li, M. K.; Xie, W. T.; Li, W.; Lin, J. Y.; Yang, J. J.; Li, X.; Su, S. J. Synergetic horizontal dipole orientation induction for highly efficient and spectral stable thermally activated delayed fluorescence white organic light-emitting diodes. *Adv. Funct. Mater.* **2022**, *32*, 2203022.

[21] Cai, M. H.; Zhang, D. D.; Xu, J. Y.; Hong, X. C.; Zhao, C. G.; Song, X. Z.; Qiu, Y.; Kaji, H.; Duan, L. Unveiling the role of Langevin and trap-assisted recombination in long lifespan OLEDs employing thermally activated delayed fluorophores. *ACS Appl. Mater. Interfaces* **2019**, *11*, 1096–1108.

[22] Lee, J. H.; Lee, S.; Yoo, S. J.; Kim, K. H.; Kim, J. J. Langevin and trap-assisted recombination in phosphorescent organic light emitting diodes. *Adv. Funct. Mater.* **2014**, *24*, 4681–4688.

[23] Kuik, M.; Koster, L. J. A.; Wetzelaer, G. A. H.; Blom, P. W. M. Trap-assisted recombination in disordered organic semiconductors. *Phys. Rev. Lett.* **2011**, *107*, 256805.

[24] Sun, L.; Sun, J. X.; Xiong, C. H.; Shi, X. H. Trap-assisted recombination in disordered organic semiconductors extended by considering density dependent mobility. *Sol. Energy* **2016**, *135*, 308–316.

[25] Zhang, D. D.; Song, X. Z.; Cai, M. H.; Kaji, H.; Duan, L. Versatile indolocarbazole-isomer derivatives as highly emissive emitters and ideal hosts for thermally activated delayed fluorescent OLEDs with alleviated efficiency roll-off. *Adv. Mater.* **2018**, *30*, 1705406.

[26] Wetzelaer, G. A. H.; Kuik, M.; Nicolai, H. T.; Blom, P. W. M. Trap-assisted and Langevin-type recombination in organic light-emitting diodes. *Phys. Rev. B* **2011**, *83*, 165204.

[27] Noguchi, Y.; Kim, H. J.; Ishino, R.; Goushi, K.; Adachi, C.; Nakayama, Y.; Ishii, H. Charge carrier dynamics and degradation

phenomena in organic light-emitting diodes doped by a thermally activated delayed fluorescence emitter. *Org. Electron.* **2015**, *17*, 184–191.
[28] Noguchi, Y.; Ninomiya, K.; Sato, K. Charge-carrier dynamics and exciton-polaron quenching studied using simultaneous observations of displacement current and photoluminescence intensity. *J. Phys. Chem. C* **2022**, *126*, 18520–18527.
[29] Juhasz, P.; Nevrela, J.; Micjan, M.; Novota, M.; Uhrik, J.; Stuchlikova, L.; Jakabovic, J.; Harmatha, L.; Weis, M. Charge injection and transport properties of an organic light-emitting diode. *Beilstein J. Nanotechnol.* **2016**, *7*, 47–52.
[30] Sem, S.; Jenatsch, S.; Sahay, P.; Züfle, S.; Schmid, M.; Brütting, W.; Ruhstaller, B. Detailed electro-optical modeling of thermally-activated delayed fluorescent OLEDs with different host-guest concentrations. *Org. Electron.* **2022**, *107*, 106553.
[31] Amorim, C. A.; Cavallari, M. R.; Santos, G.; Fonseca, F. J.; Andrade, A. M.; Mergulhão, S. Determination of carrier mobility in MEH-PPV thin-films by stationary and transient current techniques. *J. Non-Cryst. Solids* **2012**, *358*, 484–491.
[32] Shirota, Y.; Kageyama, H. Charge carrier transporting molecular materials and their applications in devices. *Chem. Rev.* **2007**, *107*, 953–1010.
[33] Kim, D.; Kwon, O.; Kim, M.; Lee, H. Charge carrier analysis via impedance spectroscopy and the achievement of high performance in CdSe/ZnS:di-[4-(N, N-di-p-tolyl-amino)-phenyl]cyclohexane hybrid quantum dot light-emitting diodes. *Org. Electron.* **2022**, *108*, 106593.
[34] Nowy, S.; Ren, W.; Elschner, A.; Lövenich, W.; Brütting, W. Impedance spectroscopy as a probe for the degradation of organic light-emitting diodes. *J. Appl. Phys.* **2010**, *107*, 054501.
[35] Shockley, W. The theory of p-n junctions in semiconductors and p-n junction transistors. *Bell Syst. Tech. J.* **1949**, *28*, 435–489.
[36] Duan, L. P.; Yi, H. M.; Xu, C.; Upama, M. B.; Mahmud, M. A.; Wang, D.; Shabab, F. H.; Uddin, A. Relationship between the diode ideality factor and the carrier recombination resistance in organic solar cells. *IEEE J. Photovolt.* **2018**, *8*, 1701–1709.
[37] Na, I.; Kim, K. J.; Kim, G. T.; Seo, Y.; Kim, Y.; Kim, Y. K.; Joo, M. K. Origin of exciplex degradation in organic light emitting diodes: Thermal stress effects over glass transition temperature of emission layer. *Appl. Phys. Lett.* **2020**, *117*, 063303.
[38] Kim, J.; Lee, T.; Kwak, J.; Lee, C. Photovoltaic characterizing method of degradation of polymer light-emitting diodes based on ideality factor and density of states. *Appl. Phys. Lett.* **2021**, *119*, 123301.
[39] Wetzelaer, G. A. H.; Koster, L. J. A.; Blom, P. W. M. Validity of the Einstein relation in disordered organic semiconductors. *Phys. Rev. Lett.* **2011**, *107*, 066605.
[40] Wetzelaer, G. J. A. H.; Kuik, M.; Blom, P. W. M. Identifying the nature of charge recombination in organic solar cells from charge-transfer state electroluminescence. *Adv. Energy Mater.* **2012**, *2*, 1232–1237.
[41] Wetzelaer, G. J. A. H.; Blom, P. W. M. Diffusion-driven currents in organic-semiconductor diodes. *npg Asia Mater.* **2014**, *6*, e110.
[42] Vandewal, K.; Tvingstedt, K.; Gadisa, A.; Inganäs, O.; Manca, J. V. Relating the open-circuit voltage to interface molecular properties of donor: acceptor bulk heterojunction solar cells. *Phys. Rev. B* **2010**, *81*, 125204.
[43] Wu, J. H.; Fischer, A.; Reineke, S. Investigating free charge-carrier recombination in organic LEDs using open-circuit conditions. *Adv. Opt. Mater.* **2019**, *7*, 1801426.
[44] Noguchi, Y.; Miyazaki, Y.; Tanaka, Y.; Sato, N.; Nakayama, Y.; Schmidt, T. D.; Brütting, W.; Ishii, H. Charge accumulation at organic semiconductor interfaces due to a permanent dipole moment and its orientational order in bilayer devices. *J. Appl. Phys.* **2012**, *111*, 114508.
[45] Lee, H.; Kim, K. J.; Moon, Y. J.; Kim, Y. K.; Kim, T. Analysis of interrelationship between efficiency and charge transport properties of green TADF organic light-emitting diodes with mixed host by impedance spectroscopy. *Org. Electron.* **2020**, *84*, 105816.
[46] Nowy, S.; Ren, W.; Wagner, J.; Weber, J. A.; Brütting, W. Impedance spectroscopy of organic hetero-layer OLEDs as a probe for charge carrier injection and device degradation. In *Proceedings of SPIE 7415, Organic Light Emitting Materials and Devices XIII*, San Diego, California, United States, 2009, pp 74150G.
[47] Han, T. H.; Kim, Y. H.; Kim, M. H.; Song, W.; Lee, T. W. Synergetic influences of mixed-host emitting layer structures and hole injection layers on efficiency and lifetime of simplified phosphorescent organic light-emitting diodes. *ACS Appl. Mater. Interfaces* **2016**, *8*, 6152–6163.
[48] Han, T. H.; Song, W.; Lee, T. W. Elucidating the crucial role of hole injection layer in degradation of organic light-emitting diodes. *ACS Appl. Mater. Interfaces* **2015**, *7*, 3117–3125.
[49] Jeon, S. K.; Lee, H. L.; Yook, K. S.; Lee, J. Y. Recent progress of the lifetime of organic light-emitting diodes based on thermally activated delayed fluorescent material. *Adv. Mater.* **2019**, *31*, 1803524.
[50] Gao, M. L.; Jang, J.; Leitner, T.; Mai, V. T. N.; Ranasinghe, C. S. K.; Chu, R.; Burn, P. L.; Pivrikas, A.; Shaw, P. E. Effect of host generation on the luminescent and charge transporting properties of solution processed OLEDs. *Adv. Mater. Interfaces* **2021**, *8*, 2100820.
[51] Shih, C. J.; Lee, C. C.; Chen, Y. H.; Biring, S.; Kumar, G.; Yeh, T. H.; Sen, S.; Liu, S. W.; Wong, K. T. Exciplex-forming cohost for high efficiency and high stability phosphorescent organic light-emitting diodes. *ACS Appl. Mater. Interfaces* **2018**, *10*, 2151–2157.
[52] Kondakov, D. Y.; Lenhart, W. C.; Nichols, W. F. Operational degradation of organic light-emitting diodes: Mechanism and identification of chemical products. *J. Appl. Phys.* **2007**, *101*, 024512.
[53] Jankus, V.; Winscom, C.; Monkman, A. P. The photophysics of singlet, triplet, and degradation trap states in 4, 4-*N,N*'-dicarbazolyl-1,1'-biphenyl. *J. Chem. Phys.* **2009**, *130*, 074501.
[54] Schmidbauer, S.; Hohenleutner, A.; König, B. Chemical degradation in organic light-emitting devices: Mechanisms and implications for the design of new materials. *Adv. Mater.* **2013**, *25*, 2114–2129.
[55] Jesuraj, P. J.; Hafeez, H.; Kim, D. H.; Lee, J. C.; Lee, W. H.; Choi, D. K.; Kim, C. H.; Song, M.; Kim, C. S.; Ryu, S. Y. Recombination zone control without sensing layer and the exciton confinement in green phosphorescent OLEDs by excluding interface energy transfer. *J. Phys. Chem. C* **2018**, *122*, 2951–2958.
[56] Lee, S.; Ha, H.; Lee, J. Y.; Shon, H. K.; Lee, T. G.; Suh, M. C.; Park, Y. Degradation mechanism of solution-processed organic light-emitting diodes: Sputter depth-profile study. *Appl. Surf. Sci.* **2021**, *564*, 150402.

Dong-Guang Zheng received his Ph.D. degree from Department of Electronics and Communications Engineering, Hanyang University, Ansan, Korea in 2021. He joined the Nanobio·Energy Materials Center at Ewha Womans University as a postdoctoral fellow to study the synthesis of perovskite material, fabrication of perovskite devices, and characterization of perovskite optoelectronic devices in the same year. He is currently conducting research work at the Hangzhou Dianzi University Information Engineering School.

Hyeon-Dong Lee received the Ph.D. degree from the Department of Materials Science and Engineering at Seoul National University, Seoul, Korea in 2023. He joined Samsung Electronics, Suwon, Korea in 2023, and is currently a staff engineer. His research focuses on the design and fabrication of organic light-emitting diodes, perovskite light-emitting diodes, and patterning method for their microarrays.

Jong-In Shim received the B.S. and M.S. degrees in Electronics from Seoul National University, Seoul, Korea, in 1983 and 1985, respectively, and the Ph.D. degree in Physical Electronics from the Tokyo Institute of Technology, Tokyo, Japan, in 1992. He is currently a Professor with the Department of Electronic and Computer Engineering, Hanyang University, Ansan, and the Head of the Semiconductor Photonics Laboratory.

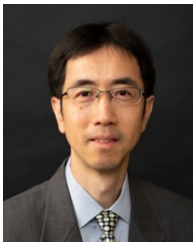

Zhiqun Lin Zhiqun Lin is a professor in the Department of Chemical and Biomolecular Engineering at the National University of Singapore. His research interests include electrocatalysis, batteries, solar energy conversion, photocatalysis, semiconductor organic–inorganic nanocomposites, multifunctional nanocrystals, conjugated polymers, block copolymers, hierarchical structure formation and assembly, and surface and interfacial properties.

Tae-Woo Lee is a Professor in the Department of Materials Science and Engineering at Seoul National University, South Korea. He received his Ph.D. in Chemical Engineering from KAIST, South Korea in 2002. He joined Bell Laboratories, USA, as a postdoctoral researcher and worked at Samsung Advanced Institute of Technology as research staff (2003–2008). He was an Associate Professor in the Department of Materials Science and Engineering at Pohang University of Science and Technology (POSTECH), South Korea, until August 2016. His research focuses on printed or soft electronics that use organic and organic-inorganic hybrid materials for flexible/stretchable displays, solid-state lighting, solar energy conversion devices, and bioinspired neuromorphic devices.

Dong Ha Kim Dong Ha Kim received his PhD degree from the Department of Fiber and Polymer Science at Seoul National University (2000). He carried out postdoctoral research at the University of Massachusetts at Amherst, USA (2000–2003) and at the Max Planck Institute for Polymer Research, Germany (2003–2005). Then, he joined the Samsung Electronics Co. in the Memory Division of Semiconductor R & D Center as a senior scientist. He assumed a faculty position in the Devision of Nanoscience at Ewha Womans University (2006). He has been elected as Ewha Fellow and Fellow of the Royal Society of Chemistry. He is currently a full professor in the Department of Chemistry and Nanoscience, the director of Nanobio·Energy Materials Center (National Research Facilities and Equipment Center) and the director Basic Sciences Research Institute (Core Research Institute) at Ewha Womans University. His research interests include the development of hybrid nanostructures for optoelectronics, next-generation battery, electro-/photo-catalysis, memory devices, display devices, and theragnosis